Mangrove Swamps of Brazil: Current Status and Impact of Sea-Level Changes

Chapter · March 2023

DOI: 10.1007/978-3-031-21329-8_3

9 authors, including:

Pedro Walfir M. Souza-Filho
VALE
32 PUBLICATIONS **616** CITATIONS
SEE PROFILE

Cesar Diniz
Solved - Soluções em Geoinformação
12 PUBLICATIONS **1,188** CITATIONS
SEE PROFILE

Luiz Cortinhas
Federal University of Pará
9 PUBLICATIONS **115** CITATIONS
SEE PROFILE

Nils E. Asp
Federal University of Pará
83 PUBLICATIONS **1,423** CITATIONS
SEE PROFILE

The Latin American Studies Book Series

José Maria Landim Dominguez · Ruy Kenji Papa de Kikuchi · Moacyr Cunha de Araújo Filho · Ralf Schwamborn · Helenice Vital *Editors*

Tropical Marine Environments of Brazil

Spatio-Temporal Heterogeneities and Responses to Climate Changes

Springer

Chapter 3
Mangrove Swamps of Brazil: Current Status and Impact of Sea-Level Changes

Pedro Walfir Martins e Souza-Filho, Cesar Guerreiro Diniz, Pedro Walfir Martins e Souza-Neto, João Paulo Nobre Lopes, Wilson Rocha da Nascimento Júnior, Luiz Cortinhas, Nils Edvin Asp, Marcus Emanuel Barroncas Fernandes, and José Maria Landim Dominguez

Abstract Mangrove swamps are found in intertidal zones along tropical and subtropical regions around the world. The spatial distribution of these coastal swamps is initially controlled by pristine landscape morphology and coastal processes related mainly to tidal ranges, currents, and salinity. This chapter presents the subdivision of the Brazilian mangrove coast based on geological, morphological, oceanographic and climatic characteristics; their spatiotemporal stability and changes in area from 1985 to 2020; sea-level changes and mangrove sedimentation evolution during the late Quaternary; and the impact of future sea-level rise. Brazilian mangroves represent the second largest area worldwide in a single country, and even in the face of a climate change scenario and a trend of relative sea-level rise over the last century, their forest area increased by 2.5%. The paleoenvironmental record of sea-level changes during the late Quaternary indicates that mangrove shorelines have a broad capacity to adjust to sea-level changes even under trajectories of sea-level rise and fall. During this century, the tendency of sea-level rise under a scenario of global warming is clear, resulting in at least four models of mangrove sedimentation adjustment based on their response to changes in hydrogeomorphic processes and pristine geological conditions.

P. W. M. e Souza-Filho (✉) · J. P. N. Lopes (✉) · W. R. da Nascimento Júnior (✉)
Vale Institute of Technology, Belém, Pará, Brazil
e-mail: pedropwm@gmail.com

P. W. M. e Souza-Filho
Federal University of Pará (UFPA), Belém, Pará, Brazil

C. G. Diniz · L. Cortinhas
Solved—Solutions in Geoinformation, Belém, Pará, Brazil

P. W. M. e Souza-Neto
University of São Paulo (USP), São Paulo, São Paulo, Brazil

N. E. Asp · M. E. B. Fernandes
Federal University of Pará (UFPA), Bragança, Pará, Brazil

J. M. L. Dominguez
Federal University of Bahia (UFBA), Salvador, Bahia, Brazil

J. M. Landim Dominguez et al. (eds.), *Tropical Marine Environments of Brazil*,
The Latin American Studies Book Series, https://doi.org/10.1007/978-3-031-21329-8_3

Keywords Coastal environments · Tidal flat · Quaternary evolution · Climate change

3.1 Introduction

Mangroves comprise mainly trees and shrubs that colonize intertidal flats in tropical and subtropical regions of the world (Perry et al. 2008). They include vegetation uniquely adapted to tidal conditions such as brackish and saltwater, periodic inundation and exposure, waves and wind, strong currents and runoff, and fine sediments (Duke et al. 1998; Tomlinson 2016). In the tidal flat zone, mangroves take the form of distinctly vegetated structures ranging from sparse shrubs to verdant closed canopy forests that occupy shorelines and upstream estuaries. Worldwide, mangroves cover a total area of ~137,700 km^2 distributed in 118 countries and territories (Giri et al. 2011; Bunting et al. 2018).

Many mangrove typologies occupy coastal plains, including deltaic, estuarine, lagoonal and open coast depositional landforms (Worthington et al. 2020). In this context, mangroves are generally limited to tidal flats that always present a narrow elevation change close to within the mean tidal level range (McKee et al. 2012). The extent of mud, mixed sediment and sand intertidal flats are conditioned by the vertical tidal range, referred to as accommodation space, whose sedimentary processes are a function of the stage of sea-level change, or maturity of the geomorphological setting, of these larger depositional systems (Woodroffe et al. 2016). The distribution of mangroves over time is controlled by the interplay of sea-level history and sediment supply, resulting in retrogradation, aggradation and progradation of coastal environments (Woodroffe 2019); vegetative stabilization; hydrology; and hydrochemical processes (Semeniuk 2018).

Along the 10,959 km of the Brazilian shoreline (IBGE 2020), mangroves present a discontinuous distribution from Orange Cape in Amapá State, latitude 4.45° N, to Laguna in Santa Catarina State, latitude 28.65° S, comprising 17 states (Fig. 3.1). The most recent mapping of Brazilian mangrove forests and shrubs quantified an area of 9627 km^2 in 2000 (Giri et al. 2011), 11,144 km^2 in 2008 (Magris and Barreto 2010), 11,072 km^2 in 2010 (Bunting et al. 2018), and 9900 km^2 in 2018 (Diniz et al. 2019). It is important to emphasize that these authors used different methods of digital image processing and mangrove mapping, which preclude accurate intercomparison of these figures. According to Bunting et al. (2018), Brazilian mangroves represent the second largest area worldwide in a single country, equivalent to 8.1% of the global mangrove area.

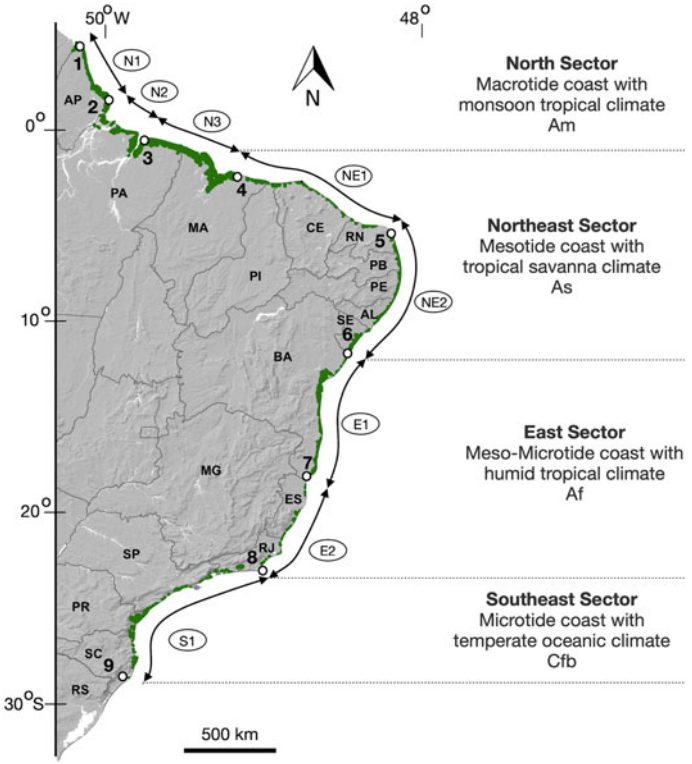

Fig. 3.1 Mangrove distribution and sectorization of the Brazilian coast based on geological, morphological, oceanographic, and climatic characteristics. N1—Subsector North 1; N2—Subsector North 2; N3—Subsector North 3; NE1—Subsector Northeast 1; NE2—Subsector Northeast 2; E1—Subsector East 1; E2—Subsector East 2; and SE1—Subsector Southeast 1. The numbers indicate the geographic boundaries of the coastal subsectors: 1—Orange Cape; 2—Norte Cape; 3—Marajó Bay; 4—Santo Amaro City, Lençois Maranhenses; 5—Calcanhar Cape; 6—Estuary of Real River; 7—Estuary of Mucuri River; 8—Arraial do Cabo; and 9—Santo Antônio Lagoon. AP—Amapá; PA—Pará; MA—Maranhão; PI—Piauí; CE—Ceará; RN—Rio Grande do Norte; PB—Paraíba; PE—Pernambuco; AL—Alagoas; SE—Sergipe; BA—Bahia; ES—Espírito Santo; RJ—Rio de Janeiro; SP—São Paulo; PR—Paraná; SC—Santa Catarina; and RS—Rio Grande do Sul

3.2 Environmental Information

To better understand the influence of geology, climate, and oceanographic conditions on mangrove distribution along the Brazilian coast, regional data and maps are required to investigate spatial variability in mangrove distribution. In this section, we present the sources of the environmental data used in this chapter.

3.2.1 Geology

The third edition of the Geological Map of South America at a scale of 1:5 M (Gomes Tapias et al. 2019) was used as the main reference to describe the geology of the Brazilian coastal zone (Fig. 3.2).

The coastal zone along the North Sector is marked by extensive Cenozoic deposits, while in the Northeast sector, these deposits occupy a narrow band bordering the coastline. In the East sector, Cenozoic and Mesozoic sedimentary rocks and Archaean high-grade metamorphic rocks crop out along the coast. The Southeast sector is

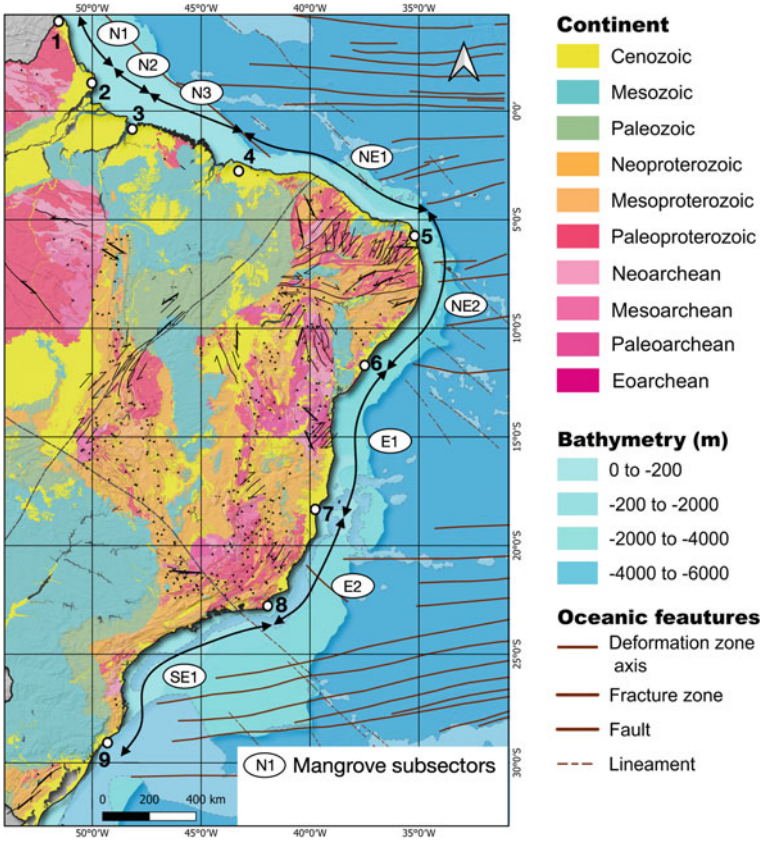

Fig. 3.2 Geological map of Brazil (Gomes Tapias et al. 2019) with indication of mangrove subsectors. N1—Subsector North 1; N2—Subsector North 2; N3—Subsector North 3; NE1—Subsector Northeast 1; NE2—Subsector Northeast 2; E1—Subsector East 1; E2—Subsector East 2; and SE1—Subsector Southeast 1. The numbers indicate the geographic boundaries of the coastal subsectors: 1—Orange Cape; 2—Norte Cape; 3—Marajó Bay; 4—Santo Amaro City, Lençois Maranhenses; 5—Calcanhar Cape; 6—Estuary of Real River; 7—Estuary of Mucuri River; 8—Arraial do Cabo; and 9—Santo Antônio Lagoon

characterized by outcrops of Proterozoic metamorphic rocks bordering the coastal zone.

3.2.2 Climate

Figure 3.3 shows the Köppen climate class distribution for Brazil from Alvares et al. (2013). Air temperature, precipitation, evaporation, and relativity humidity over the continent are shown in Fig. 3.4.

The climate in the North sector is defined as tropical monsoon (Am) (Fig. 3.3), with average annual precipitation higher than 1800 mm, air temperature ranging from 24 to 33 °C, evaporation between 1000 and 1600 mm per year, and air relativity humidity between 80 and 90%. Figure 3.4 shows the spatial distribution of these meteorological variables. The Northeast sector is characterized as tropical savanna (As) (Fig. 3.3), with average annual precipitation ranging from 800 to 1600 mm, air temperature ranging from 24° to 35 °C, evaporation between 1600 and 2800 mm per year, and air relativity humidity between 70 and 85% (Fig. 3.4). In the East sector, the climate is defined as humid tropical without a dry season (Af) (Fig. 3.3), with average annual precipitation ranging from 1000 to 1600 mm, air temperature ranging from 20 to 33 °C, evaporation between 1000 and 1600 mm per year, and air relativity humidity between 75 and 85% (Fig. 3.4). The climate in the Southeast sector is defined as temperate oceanic (Cfb) (Fig. 3.3), with average annual precipitation ranging from 1200 to 2000 mm, air temperature ranging from 18 to 29 °C, evaporation between 800 and 1400 mm per year, and air relativity humidity between 75 and 85% (Fig. 3.4).

3.2.3 Oceanographic Parameters

Figure 3.5a shows the spatial variation in the M2 tidal amplitude from the AVISO Global Tide Model with a horizontal resolution of 0.0625°. Figure 3.5b shows the spatial variation in the significant wave height generated from the ECMWF (ERA5) reanalysis for the global climate and weather for the 1979 to 2021 period (Hersbach et al. 2020).

Figure 3.6 shows the distribution of mean sea surface temperature, salinity, chlorophyll and particulate organic carbon (POC) for the western South Atlantic Ocean. The World Ocean Atlas 2018 (WOA2018) was used for sea surface temperature and salinity at the ocean surface (Locarnini et al. 2019; Zweng et al. 2018). This climatology used in situ measurements to generate a mean field for the period between 1955 and 2017 with a horizontal resolution of 0.25°. POC from 1997 to 2021 (Stramski et al. 2008) and chlorophyll type 2 from 2002 to 2012 (Doerffer and Schiller 2007) were derived from the Global Color project – GLOBCOLOR (https://www.globcolor.info/).

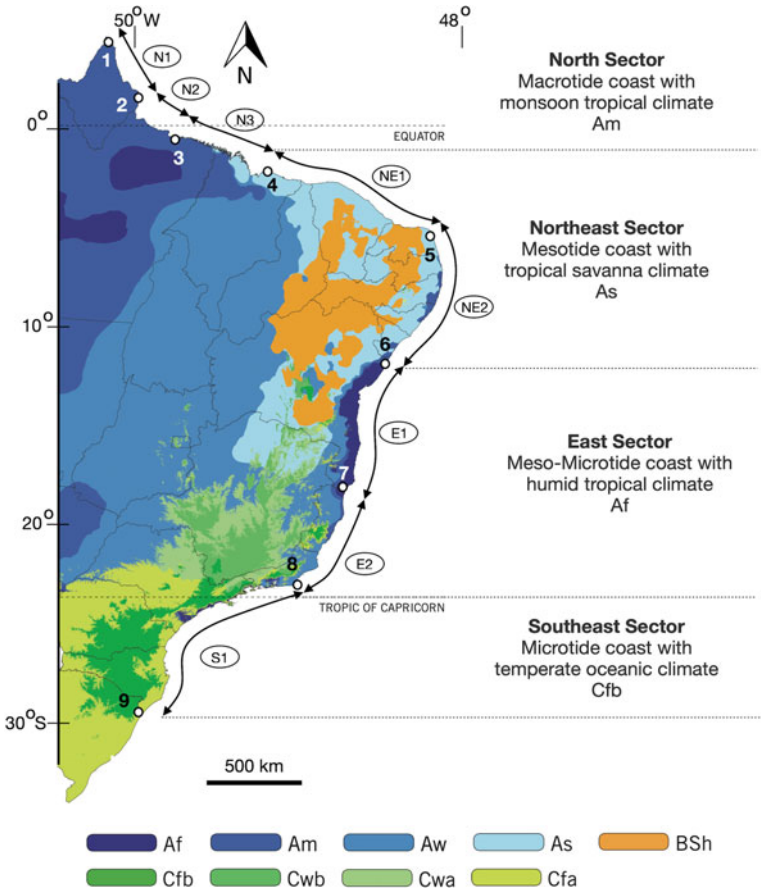

Fig. 3.3 Köppen climate classification map for Brazil (Alvares et al. 2013) with indication of mangrove subsectors. N1—Subsector North 1; N2—Subsector North 2; N3—Subsector North 3; NE1—Subsector Northeast 1; NE2—Subsector Northeast 2; E1—Subsector East 1; E2—Subsector East 2; and SE1—Subsector Southeast 1. The numbers indicate the geographic boundaries of the coastal subsectors: 1- Orange Cape; 2—Norte Cape; 3—Marajó Bay; 4—Santo Amaro City, Lençois Maranhenses; 5—Calcanhar Cape; 6—Estuary of Real River; 7—Estuary of Mucuri River; 8—Arraial do Cabo; and 9—Santo Antônio Lagoon

The North sector is characterized by a macrotidal regime with spring tides ranging from 3 m to 6.6 m and a mean significant wave height reaching up to 0.5 m (Fig. 3.5). The average sea surface temperature is higher than 27 °C, with higher concentrations of chlorophyll *a* (> 1300 mg.m^{-3}), salinity is lower than 35, and POC is higher than 40 mol.m^{-3} (Fig. 3.6).

The Northeast sector has a mesotidal regime with a spring tidal range reaching up to 3.8 m and a mean significant wave height reaching 1.2 m (Fig. 3.5). The sea surface temperature is higher than 27 °C and the concentrations of chlorophyll *a*,

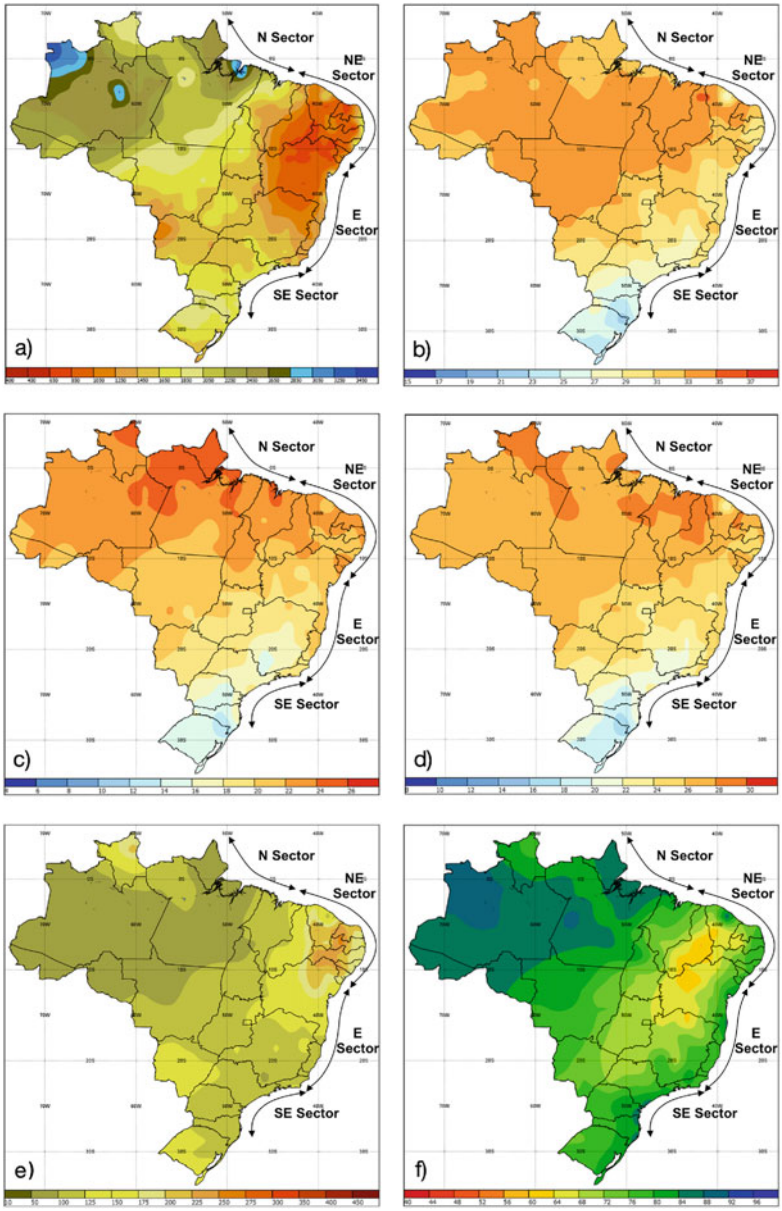

Fig. 3.4 Climatological normals for Brazil (1990–2020). **a** Accumulated average annual rainfall in mm, **b** maximum annual air temperature in °C, **c** minimum annual air temperature in °C, **d** average annual air temperature in °C, **e** accumulated average annual evaporation in mm, and **f** average annual relative humidity in %. Data source: Brazilian Institute of Meteorology—INMET, (https://clima.inmet.gov.br/NormaisClimatologicas/)

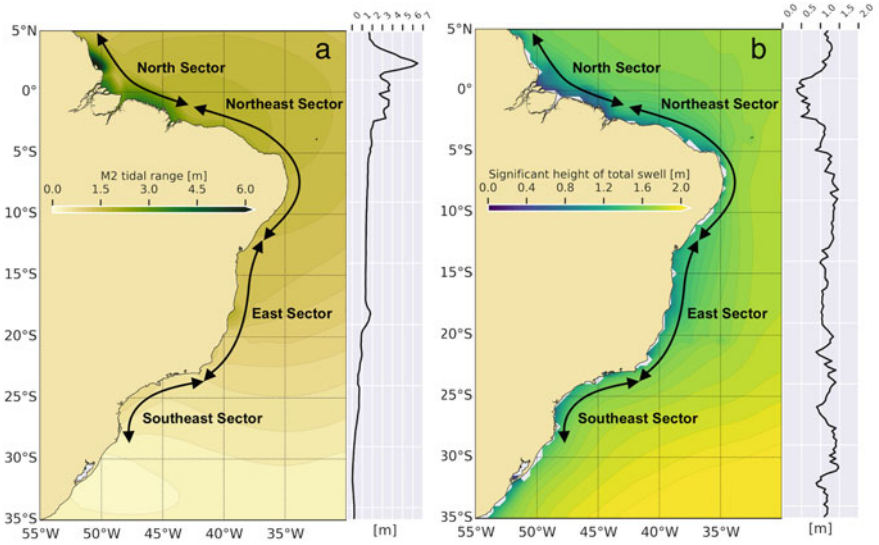

Fig. 3.5 **a** Alongshore M2 tidal amplitude variation *Source* AVISO Global Tide Model https://www.aviso.altimetry.fr/en/data/products/auxiliary-products/global-tide-fes.html. **b** Alongshore spatial variation in the significant wave height (Hersbach et al. 2020)

salinity, and particulate organic carbon range from 8 to 100 mg.m^{-3}, 24 to 37.5, and 20 to 30 mol.m^{-3}, respectively (Fig. 3.6).

The East Sector is characterized by a meso- to microtidal regime with spring tides ranging from 1.6 to 2.9 m and a mean significant wave height reaching 1.5 m (Fig. 3.5). Sea surface temperature ranges from 21° to 27 °C with concentrations of chlorophyll *a* lower than 100 mg.m^{-3}, salinity of approximately 36, and POC ranging from 20 to 50 mol.m^{-3} (Fig. 3.6).

The Southeast sector is characterized by a microtidal regime with spring tides ranging from 0.8 to 1.7 m and a mean significant wave height reaching 1.5 m (Fig. 3.5). Sea surface temperature ranges from 20° to 24 °C with concentrations of chlorophyll *a*, salinity, and POC ranging from 8 to 100 mg.m^{-3}, 35 to 36, and 20 to 30 mol.m^{-3}, respectively (Fig. 3.6).

3.3 Mangrove Spatial Distribution Along the Brazilian Coast

The mangrove cover area used in this chapter was generated from the Mapbiomas Project (https://mapbiomas.org). The mangrove extension was mapped in the Google Earth Engine (GEE) managed pipeline to compute the annual status of Brazilian mangroves from 1985 to 2020. Mangrove forests were identified from the use of

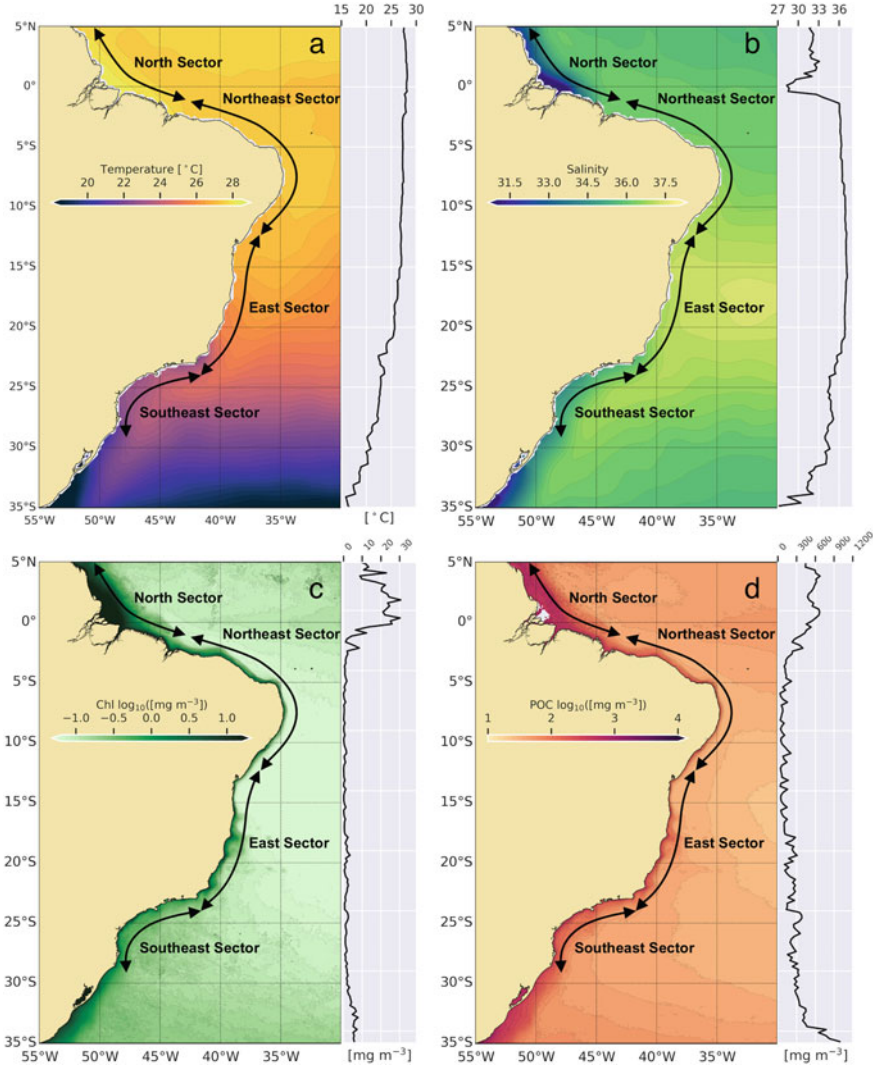

Fig. 3.6 Spatial distribution of: **a** sea surface temperature. **b** Salinity. **c** Chlorophyll *a*. **d** Particulate organic carbon along the Brazilian coast. *Data Source* **a**, **b**) https://www.ncei.noaa.gov/products/world-ocean-atlas; **c**, **d**) https://www.globcolor.info/

a spectral index, the Modular Mangrove Recognition Index (MMRI), which was specifically designed to better discriminate mangrove forests from the surrounding vegetation (Diniz et al. 2019).

The integration of mangrove mapping with geological, oceanographic, and climatic characteristics allowed us to divide the Brazilian coast into five large sectors: North, Northeast, East, Southeast, and South (Figs. 3.1, 3.2, and 3.3). Table 3.1

presents the boundaries and synthesizes the main climatic and oceanographic characteristics of each sector. This division integrates aspects of former classifications proposed by Schaeffer-Novelli et al. (1990), Knoppers et al. (1999), Souza-Filho et al. (2005), Dominguez (2009), Klein and Short (2016), Lessa et al. (2018), and Silva and Torres (2021).

Along the Brazilian coast, mangroves are found in different environmental settings. For instance, on open coasts, associated with wide tidal flats, such as on the Amapá coast, mangrove fringes prograde seaward over mud banks (Allison et al. 1995). This pattern contrasts with the sheltered open jagged coast with macrotidal

Table 3.1 Geographic boundaries and meteorological and oceanographic characteristics of the Brazilian mangrove sectors

Coastal sectors	North sector	Northeast sector	East sector	Southeast sector
Sector boundaries	From Oiapoque (AP) to Cabo Orange to Santo Amaro (MA)	From Santo Amaro (MA) to the estuary of the Real River (SE)	From the estuary of the Real River (SE) to Arraial do Cabo (RJ)	From Arraial do Cabo (RJ) Santo Antônio Lagoon (SC)
Latitude	From 3.847621° N to 2.498599° S	From 2.498599° to 11.44249° S	From 11.44249° to 23.014227° S	From 23.014227° to 28.519253° S
Longitude	From 51.836322° to 43.250772° W	From 43.250772° to 37.340266° W	From 37.340266° to 42.000135° W	From 42.000135° to 48.773824°W
Köppen Classification	Monsoon tropical climate (Am)	Tropical savanna climate (As)	Humid tropical climate (Af)	Temperate oceanic climate (Cfb)
Air temperature (°C)	24–33°	24–35°	20–33°	18–29°
Average annual precipitation (mm)	> 1800	800–1660	1000–1600	1200–2000
Evaporation (mm/year)	1000–1600	1600–2800	1000–1600	800–1400
Air relative humidity (%)	80–90	70–85	75–85	75–85
Tidal range (m)	3.5–6.6	2.2–3.8	1.6–2.9	0.8–1.7
Significant wave height (m)	Up to 0.5	Up to 1.2	Up to 1.5	Up to 1.5
Sea surface temperature (°C)	> 27°	> 27°	21–27°	20–24°
Chlorophyll *a* ($mg.m^{-3}$)	> 1300	8–100	< 100	8–100
Salinity	< 35	24–37.5	36	35–36
Particulate organic carbon ($mol.m^{-3}$)	> 40	20–30	20–50	20–30

estuaries, characteristic of the Pará and Maranhão states, where mangroves developed on the largest tidal mudflats of Brazil, behind dune-beach sandy barriers (Souza-Filho et al. 2009). Estuarine mangroves occur in northeastern and southeastern Brazil along the margins of tidal channels located in coastal embayments (Rodrigues 2014), while mangroves in lagoons and bays have developed behind spits and other sandy barriers, such as Sepetiba Bay in Rio de Janeiro State (Dadalto et al. 2022). Mangroves also occur in delta plains, for example, in the São Francisco delta, behind sandy barriers (Dominguez and Guimarães 2021). The following sections present detailed descriptions of the major mangrove sectors present along the Brazilian coast, emphasizing the long-term sedimentation patterns and their stratigraphic framework and showing the five major types of mangroves occurring in Brazil: open coast, sheltered open coast, estuary, delta, and bay-lagoon. Although these five categories do not encompass all types of occurrences, they represent the most important environments where mangroves are found along the coast of Brazil.

3.3.1 The North Sector

This sector, on the Amazonian coast, is 4048 km long and forms an embayed shoreline and runs from the estuary of the Oiapoque River on the Orange Cape, Amapá State, to Santo Amaro City, in the western boundary of the Lençóis Maranhenses dune field in Maranhão State (Fig. 3.1). This is a subsiding coast (Rossetti 2014; Souza-Filho 2000), and it is marked by the presence of the Amazon River mouth and 24 other estuaries. Although this sector is subjected to rising sea levels, the coastal zone is prograding (Souza-Filho et al. 2009).

Three subsectors were identified (Fig. 3.7):

Subsector N1 extends from the mud banks of Orange Cape to Norte Cape located in the North Channel of the Amazon River (Fig. 3.7). This coastal region is strongly influenced by the Amazon sediment plume, which extends northwestward, creating extensive mud flats prograding in an open coast (Fig. 3.7a) dissected mainly by estuaries draining a wet-muddy-humid hinterland (Allison et al. 1995; Batista et al. 2009). According to Schaeffer-Novelli et al. (1990), this subsector is characterized by homogeneous forests dominated by black mangrove, *Avicennia,* where *Pterocarpus* is sometimes found. The mangrove trees grow on an open coast forming an extensive and continuous mangrove belt 2 km wide, extending up to 30 km upstream in the estuaries. *Rhizophora* occurs in the estuarine portions of rivers close to the shoreline.

Subsector N2 is bounded by the mouths of the Amazon and Tocantins Rivers and Marajó Bay, comprising Marajó Island and a cluster of low-lying islands in the Amazon River mouth. This subsector presents evidence of tectonic activity contemporaneous with sediment deposition during the mid- to late Quaternary (Rossetti et al. 2008). Mangrove vegetation is restricted to muddy sandflats around these islands, forming fringes up to 4 km in width (França and Souza-Filho 2003, 2006; França et al. 2007). Mangroves occur mixed with freshwater swamp vegetation due to the high discharges of the Amazon and Tocantins Rivers (Schaeffer-Novelli et al. 1990).

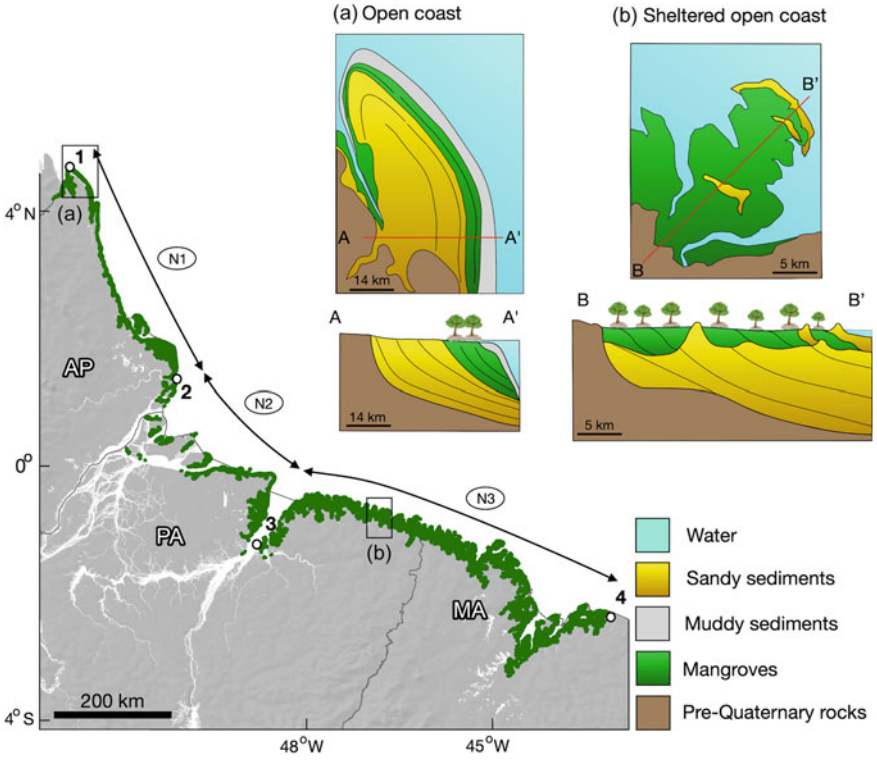

Fig. 3.7 The Brazilian Mangrove North Sector also depicts sedimentary environments and stratigraphic frameworks reflecting long-term sedimentation patterns. **a** open coast mangrove type typical of the Orange Cape mud flats common in Subsector N1. **b** sheltered open coast mangrove type typical of the macrotidal sandy dune-beach barriers of the Bragança coastal plain in Subsector N3. 1—Orange Cape; 2—North Cape, 3—Marajó Bay, and 4—Santo Amaro City

Avicennia germinans occur at higher elevations and lower salinity areas. Low salt tolerance might explain the restriction of *R. racemosa* and *R. harrisonii* to the Marajó Bay region (Menezes et al. 2008).

Subsector N3 comprises the Amazon macrotidal mangrove coast (Souza-Filho 2005) and extends from Marajó Bay to Lençóis Maranhenses (Fig. 3.7). Seventeen macrotidal estuaries occur along this embayed and jagged coast, comprising the largest continuous mangrove belt in the world with an area of approximately 7500 km^2. In this region, the mangrove belt reaches up to 23 km in width (Nascimento et al. 2013; Souza-Filho 2005). This subsector is characterized by wide intertidal mud and sandflats developed under a subsiding macrotidal barrier estuarine system (Souza-Filho et al. 2009), characterizing a sheltered open coast (Fig. 3.7b). *Rhizophora mangle* is the most widely distributed mangrove species, dominating upstream riverbanks and back basins in macrotidal estuaries and downstream riverbanks and open coast fringe forests over muddy tidal flats. *Rhizophora mangle* stands

are backed by *Avicennia germinans* and *A. schaueriana,* and *Laguncularia racemosa* stands at higher elevations and less inundated areas under less saline conditions (Menezes et al. 2008), while saline muddy sandflats are colonized by *Spartina* (Schaeffer-Novelli et al. 1990).

3.3.2 The Northeast Sector

The Northeast Sector is 2047 km long and extends from Santo Amaro City, Lençóis Maranhenses, to the estuary of the Real River, Sergipe State (Fig. 3.8). This Brazilian coastal sector has received the smallest volume of sediments in recent geological time as a result of the small size of the drainage basins, low relief and low precipitation (Dominguez 2009). Geomorphologically, the Northeast Sector is marked by coastal cliffs up to ~ 40 m high carved into the Miocene Barreiras Formation (Peulvast et al. 2006; Rossetti et al. 2013). Quaternary accumulations in this sector include active and inactive dune and transgressive aeolian sand sheets, Pleistocene and Holocene beach deposits, beach rocks and estuarine deposits (Bezerra et al. 2003; Barreto et al. 2006). This sector is marked locally by the presence of the deltas of the Parnaíba and São Francisco Rivers on the western and southern boundaries, respectively. Between these two deltas, 11 mesotidal estuaries occur (Lessa et al. 2018).

Two subsectors were identified in this sector (Fig. 3.8):

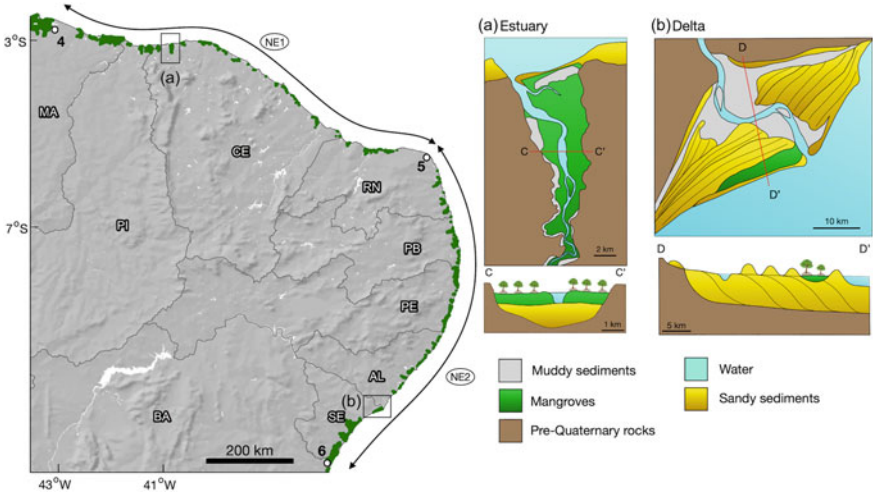

Fig. 3.8 The Brazilian Mangrove Northeast Sector also depicts sedimentary environments and stratigraphic frameworks reflecting long-term sedimentation patterns. **a** estuarine mangrove type model exemplified by the mesotidal estuarine system of the Acaraú River in Ceará State (Subsector NE1). **b** wave-dominated deltaic mangrove type exemplified by the São Francisco Delta (Subsector NE2). 4—Santo Amaro City, 5—Calcanhar Cape, and 6—Estuary of Real River

Subsector NE1 extends from Santo Amaro City to Calcanhar Cape in Rio Grande do Norte State (Fig. 3.8). The west–east-oriented subsector is marked by intense east–west littoral drifts with sand accumulating in narrow sandy barriers at the foot of sea cliffs and at the mouth of mesotidal estuaries located behind transgressive beach-dune fields (Hesp et al. 2009; Vital et al. 2016). Figure 3.8a illustrates the spatial distribution of this kind of mangrove depositional system developed under estuarine mesotidal conditions in the Acaraú River in Ceará State. Mangroves are poorly developed along this coast segment due to the lack of freshwater and prolonged droughts (Schaeffer-Novelli et al. 1990) and reduced sediment input to build a coastal plain. High salt concentrations limit mangrove development that is restricted to estuarine channels, dominated by *Rhizophora mangle* followed by *Avicennia schaueriana* (Costa et al. 2017).

Subsector NE2 extends from the Calcanhar Cape to the Real River estuary (Fig. 3.8). This north–south oriented subsector is also marked by sea cliffs carved into the Miocene Barreiras Formation (Rossetti et al. 2013) and extensive active and inactive transgressive dune fields (Bezerra et al. 2001). These dunes extend up to 3 km inland, reaching heights of up to 80–120 m. Beach rocks are discontinuously exposed along the shoreline. They are oriented nearly parallel to the shoreline, a few kilometers long, with thicknesses from 10 cm to 3 m and widths from 2 to 50 m. Most of them are located in the present intertidal zone, which is characterized by the presence of gently seaward-dipping stratification (Ferreira et al. 2018; Vieira et al. 2017). Due to the high wave energy in this coastal subsector, mangroves are restricted to estuarine channels and behind coastal barriers, such as the delta of the São Francisco River, where mangroves occur behind sand spits (Fig. 3.8b). In tidal flat deposits, basin forests may contain either *Avicennia* or *Laguncularia* or mixed stands of both species. Either *Rhizophora* or *Laguncularia* may appear as pioneering species, while *Spartina* may occur in some accretionary deposits near the shoreline (Schaeffer-Novelli et al. 1990).

3.3.3 The East Sector

This 1804 km long sector extends from the estuary of the Real River (Sergipe State) to the Arraial do Cabo promontory in Rio de Janeiro State (Fig. 3.9). According to Dominguez (2009), along this sector, the major escarpment typical of rifted passive continental margins has retreated hundreds of kilometers from the coastal zone, creating large drainage basins. Furthermore, this coastal sector is characterized by classical examples of wave-dominated deltas, such as Jequitinhonha, Doce and Paraíba do Sul (Dominguez et al. 1987). In between these major deltas, coastal cliffs carved into the Barreiras formation occur locally. This sector is marked by the presence of the Todos os Santos, Camamu and Vitória bays, in addition to the estuaries of smaller rivers (Lessa et al. 2018).

The east sector can be subdivided into two subsectors:

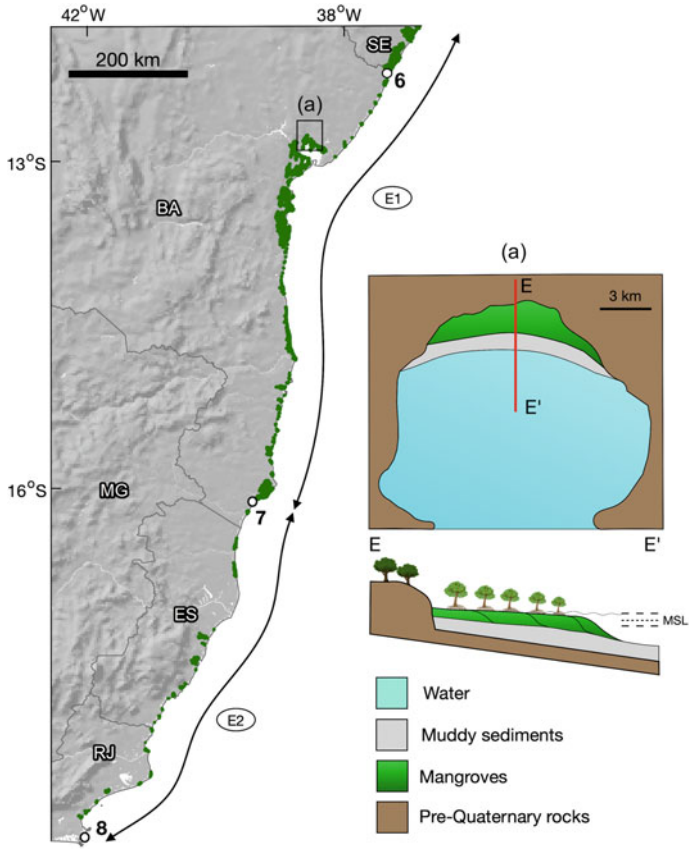

Fig. 3.9 The Brazilian Mangrove East Sector also depicts sedimentary environments and stratigraphic frameworks reflecting long-term sedimentation patterns. **a** bay-lagoon delta mangrove delta type exemplified by the mesotidal Todos os Santos Bay in Bahia State. 6—Estuary of the Real River, 7—Estuary of the Mucuri River and 8—Arraial do Cabo

Subsector E1 is situated between the estuaries of the Real and Mucuri Rivers (Fig. 3.9). Siliciclastic sediments occur along a narrow band bordering the shoreline extending to the 15 isobaths, while the rest of the shelf is characterized by carbonate sedimentation (Dominguez et al. 2013; Halla et al. 2020). Extensive mangroves occur associated with the estuaries of major rivers and strand plains and in the large bays present in this sector, such as Camamu and Todos os Santos Bay (Fig. 3.9a). This ecosystem has a fringe physiognomy with a low bearing that contains *Laguncularia racemosa*, *Rhizophora mangle* and *Avicennia schaueriana* (Freitas et al. 2002).

Subsector E2 extends from the estuary of the Mucuri River (Bahia State) to Arraial do Cabo (Rio de Janeiro State) (Fig. 3.9). This subsector is characterized by the two largest wave-dominated deltas of Brazil, the Doce and Paraíba do Sul deltas, with sea cliffs carved into the Barreiras Formation present in between (Dominguez et al. 1987).

Interestingly, no major occurrences of mangrove forests are associated with these two deltas that do not present significant intrusion of salt water into the channel. The largest mangrove forest of this subsector occurs in Vitória Bay, with the dominance of *Rhizophora mangle* and *Laguncularia racemosa* (Barbirato et al. 2021). In this sector, mangroves occur mainly along the margins of microtidal estuaries.

3.3.4 The Southeast Sector

The Southeast Sector extends for 2443 km from Arraial do Cabo (Rio de Janeiro State) to Laguna (Santa Catarina State) (Fig. 3.10). Geomorphologically, this sector is characterized as a high-relief coast (up to 1000 m), where the Mantiqueira and do Mar mountain ranges (Archaean and Proterozoic rocks) border the coastline (Almeida and Carneiro 1998). This high relief near the coast forces the major drainages to flow toward the hinterland, resulting in an overall small sediment load to the coast (Dominguez 2009). Tectonic uplift at the end of the Cretaceous followed by gravitational collapse produced a series of grabens oriented subparallel to the coast, which were flooded by the sea and created a number of bays and large estuaries, which characterizes this sector (Dominguez 2009). This Southeast Sector is marked by the presence of barrier-island lagoon systems and bays such as Guanabara, Santos and Paranaguá. The tidal flats occur inside bays and lagoons behind beach-dune barrier systems (Fig. 3.10a).

In this sector, the largest mangrove forests occur in Guanabara, Sepetiba, Santos and Paranaguá Bays. The mangrove fringes of these regions are dominated by *Rhizophora mangle,* followed by *Laguncularia racemosa*, *Avicennia germinas* and *A. schaueriana* (Schaeffer-Novelli et al. 1990). The Santo Antônio Lagoon located in the region of Laguna in Santa Catarina State is the southern limit of occurrence of mangroves in the western Atlantic Ocean (Soares et al. 2012).

3.4 Mangrove Changes from 1985 to 2020

Along the Brazilian coast, mangrove forests exhibited a net increase from 9564 km^2 in 1985 to 9800 km^2 in 2020, which represents just 2.5% of the total mangrove area. This total area increased by 6.4% from 1985 to 2002, decreasing afterwards by 3.8% from 2003 to 2020 (Fig. 3.11). Diniz et al. (2019) defined these two periods as accretionary and erosive, respectively. Here, we use this timeline to describe the mangrove dynamics along the coastal subsectors. Figure 3.11 presents the quantification of the mangrove area per sector for 1985, 2002, 2003, and 2020, whereas Fig. 3.12a presents the mangrove area changes per subsector for the same years. The stable mangrove area representing the unchanged area during the analysis period and mangrove area gain (expansion) and mangrove area loss (reduction) for the 1985–2002 and 2003–2020 periods are presented in Figs. 3.12b, c, respectively.

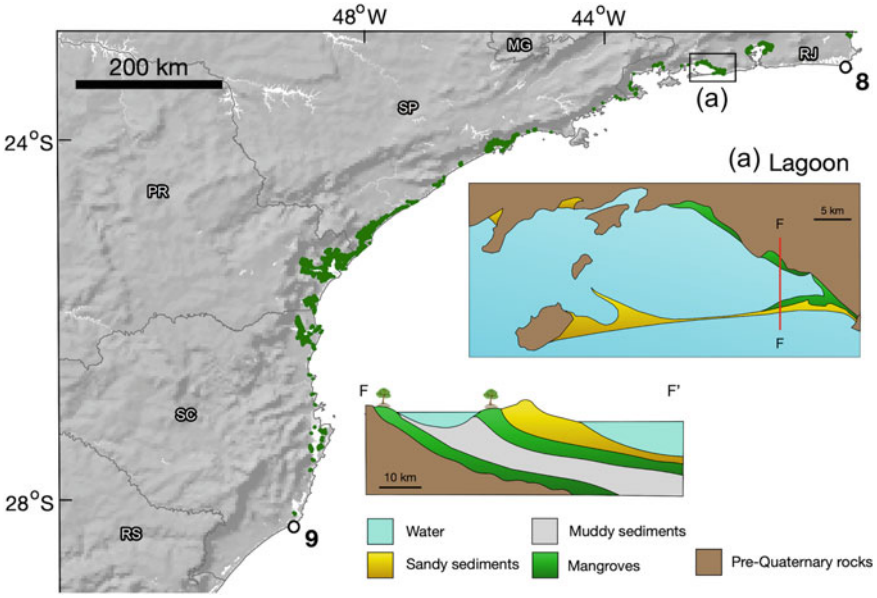

Fig. 3.10 The Brazilian Mangrove Southeast Sector also depicts sedimentary environments and stratigraphic frameworks reflecting long-term sedimentation patterns. **a** bay/lagoon mangrove type model exemplified by the Sepetiba barrier island system in the State of Rio de Janeiro. 8—Estuary of the Mucuri River and 9—Santo Antônio Lagoon in Santa Catarina State

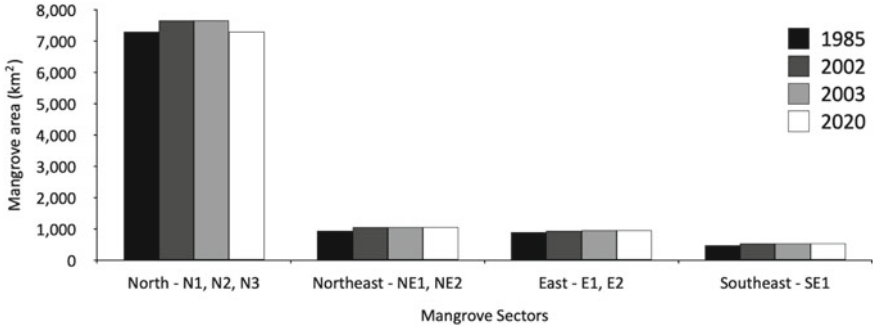

Fig. 3.11 Mangrove area per coastal sector for 1985, 2002, 2003, and 2020

In the North Sector, mangrove forest occupied an area of 7283 km^2 in 2020, which represents 74.3% of the Brazilian mangroves. From 1985 to 2020, the total mangrove area in this sector remained constant.

Subsector N1 comprised 8.4% of the Brazilian mangroves in 2020. From 1985 to 2020, mangrove forest decreased by 3.3%. The rate of change, however, was not uniform. From 1985 to 2002, the mangrove forest increased by 18.2%, and from 2003 to 2020, it decreased by 17.9%. Between 1985 and 2002, 665 km^2 of mangrove forest

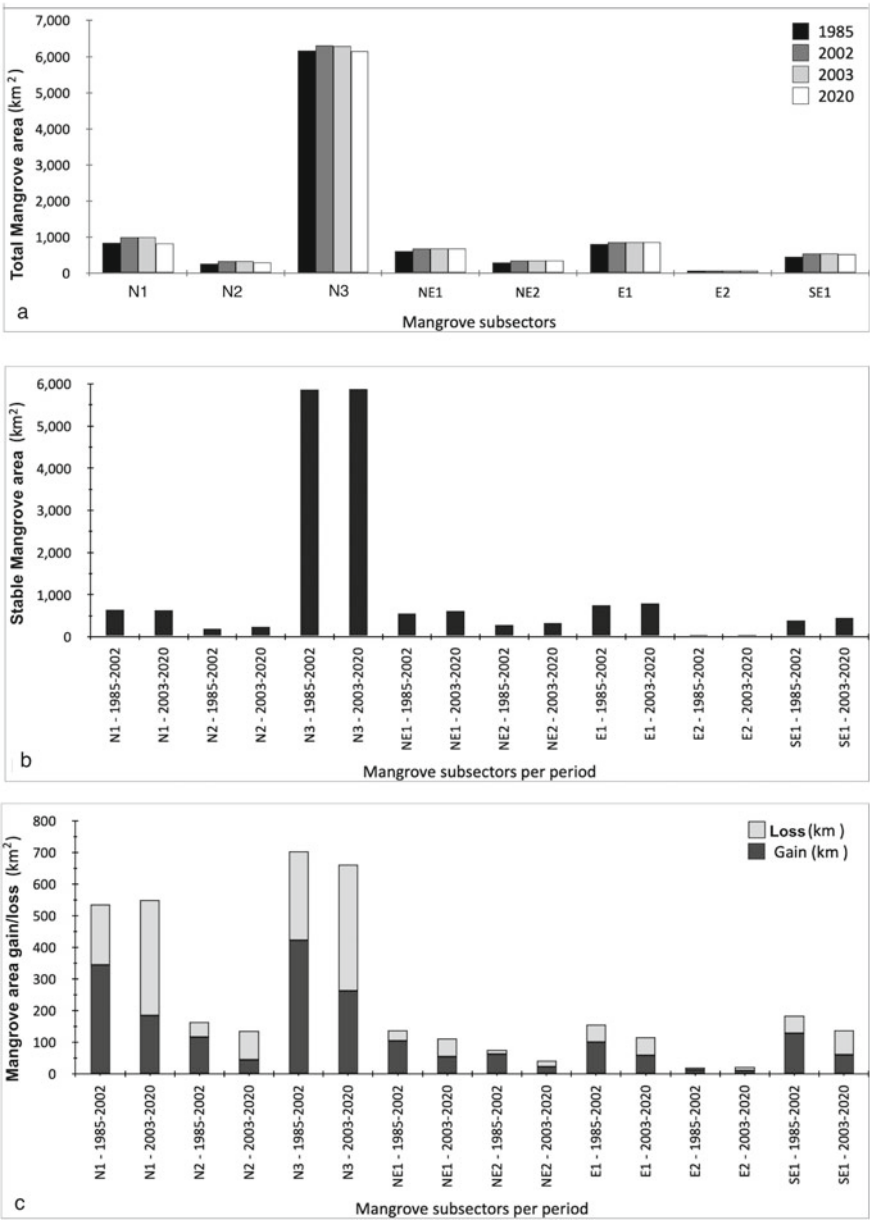

Fig. 3.12 **a** Total mangrove area per subsector for 1985, 2002, 2003, and 2020. **b** Stable mangrove area and **c** mangrove area gain and loss in the 1985–2002 and 2003–2020 periods

remained stable in this subsector with a gain of 345 km^2 and a loss due to coastal erosion of 190 km^2. However, from 2003 to 2020, the stable mangrove forest area remained at approximately 642 km^2 with gains of 185 km^2 and losses of 366 km^2 (Fig. 3.12).

Subsector N2 accounted for 3.1% of the Brazilian mangrove forest area in 2020. In this subsector, the mangrove area enlarged from 267.6 km^2 in 1985 to 300.5 km^2 in 2020, representing a net gain of 12.3%. Stable mangrove areas occupied 220 km^2 and 255 km^2 during the 1985–2002 and 2003–2020 periods, respectively. This subsector presents the same behavior as Subsector N1, with the largest gain occurring during 1985–2002 (117 km^2) and the largest loss occurring during the 2003–2020 period (91 km^2) (Fig. 3.12).

Subsector N3, which comprises the largest mangrove belt in the world (Souza-Filho 2005), had a total area of 6155 km^2 in 2020. This area represents 62.8% of the Brazilian mangrove forests. Along this sector, the mangrove area also decreased from 6160 km^2 in 1985 to 6155 km^2 in 2020, a reduction of 0.1%. The stable mangrove area was 5878 km^2 from 1985 to 2002 and 5892 km^2 from 2003 to 2020, with the largest gain occurring in the first period (422 km^2) and the largest loss in the second period (399 km^2) (Fig. 3.12).

In the Northeast Sector, mangrove areas totaled 1045 km^2 in 2020, which corresponds to 10.7% of the Brazilian mangroves. In general, the mangrove forest area increased by 13.1% from 1985 to 2020 (Fig. 3.11).

Subsector NE1 contained 7% of the total mangrove area of Brazil in 2020. In this subsector, the mangrove area increased continuously from 612.3 km^2 to 681.6 km^2 from 1985 to 2020, exhibiting a pattern completely different from that in the North Sector. From 1985 to 2002, 579.7 km^2 of mangrove area remained stable, with a gain of 105.4 km^2 and a loss of 33 km^2. However, from 2003 to 2020, the stable mangrove forest area increased to 627 km^2, with a gain of 54.3 km^2 and a loss of 58.3 km^2 (Fig. 3.12).

Subsector NE2 comprised 3.7% of the total Brazilian mangrove forests in 2020. Its mangrove area also increased continuously from 311.4 km^2 in 1985 to 363.4 km^2 in 2020, representing a gain of 15.8%. The stable mangrove area was 220 km^2 and 255 km^2 during the 1985–2002 and 2003–2020 periods, respectively. This subsector presented the same behavior as Subsector NE1, with a gain of 63.4 km^2 and a loss of 14.2 km^2 during the 1985–2002 period and similar gains (22.4 km^2) and losses (21 km^2) during the 2003–2020 period (Fig. 3.12).

The East Sector encompassed 946.2 km^2 of mangrove forest in 2020, representing 9.7% of the Brazilian mangroves. The mangrove area increased by 6.3% from 1985 to 2020, although a small decrease of 0.3% occurred from 2003 to 2020 (Fig. 3.11).

Subsector E1 comprised 8.9% of the Brazilian mangrove forests in 2020. In this subsector, the mangrove area increased from 820 km^2 in 1985 to 869.7 km^2 in 2020, representing a net gain of 6.1%. The stable mangrove area occupied 764.2 km^2 and 812 km^2 during the 1985–2002 and 2003–2020 periods, respectively. This subsector exhibited the same behavior as Subsectors NE1 and NE2, with gains (101 km^2) larger than losses (55.8 km^2) during 1985–2002 and equivalent gains (57.8 km^2) and losses (59 km^2) during 2003–2020 (Fig. 3.12).

Subsector E2 had the smallest mangrove area of Brazil, with 76.5 km^2 in 2020, representing only 0.8% of the total mangrove forest of Brazil. Along this sector, the mangrove area increased by 9.3% from 1985 to 2020. The stable mangrove area was similar during the two periods of investigation (63.3 km^2 during 1985–2002 and 66.2 km^2 during 2003–2020), with the largest gain (13.3 km^2) and smaller loss (6.6 km^2) occurring during 1985–2002 and similar gains (10.3 km^2) and losses (11.9 km^2) occurring during the 2003–2020 period (Fig. 3.12).

The Southeast Sector has an area of 525.6 km^2 of mangrove forest, which represents 5.4% of the total Brazilian area. From 1985 to 2020, the mangrove area increased from 467.4 km^2 in 1985 to 525 km^2 in 2020. However, from 2003 to 2020, a small decrease of 3.2% from 543 km^2 to 525.6 km^2 was documented. Between 1985 and 2002, the stable mangrove area totaled 412 km^2, with a gain of 129.2 km^2 and a loss of approximately 55 km^2. However, from 2003 to 2020, the mangrove stable area increased to 465.4 km^2, with gains of 60.2 km^2 and losses of 77.6 km^2 (Fig. 3.12).

Summing up the data presented above indicates that overall, the mangrove area in Brazil remained stable during the 1985–2020 period in all sectors, although it exhibited changes of a small magnitude. An increase of just 2.5% in the total mangrove area in Brazil was documented.

3.5 Impacts of Sea-Level Changes in the Brazilian Mangroves

3.5.1 Sea-Level Changes and Evolution of Mangrove Sedimentation Evolution During the Holocene

A number of papers have discussed the impact of future sea-level changes (Schaeffer-Novelli et al. 2002; Ellison 2015; Duncan et al. 2018) on the sedimentation, morphology, and development of mangrove ecosystems (Cohen et al. 2015; Woodroffe et al. 2016; Woodroffe 2019).

One way to investigate the impact of future sea-level changes in mangrove forests is to assess how tidal flats colonized by mangroves have responded to the rise in sea- level since the Last Glacial Maximum (LGM). Different responses of mangrove shorelines to sea-level change were discussed by Woodroffe (2018), including drowning, backstepping, catch-up, keep-up, progradation and emergence. The past trajectories of the mangrove shorelines depend on the Holocene sea-level history. Along the Atlantic South American coast, it is possible to observe two distinct Holocene sea-level histories: (i) a 3–4-m relative sea-level drop since the Mid-Holocene (Angulo et al. 2006) observed along most of the northeastern to southern Brazilian coast and (ii) a continuous sea-level rise during the Holocene along the northern coast of Brazil and the Caribbean (Khan et al. 2015) (Fig. 3.13). These differences are a direct effect of Greenland ice sheet (GIS) and Antarctic

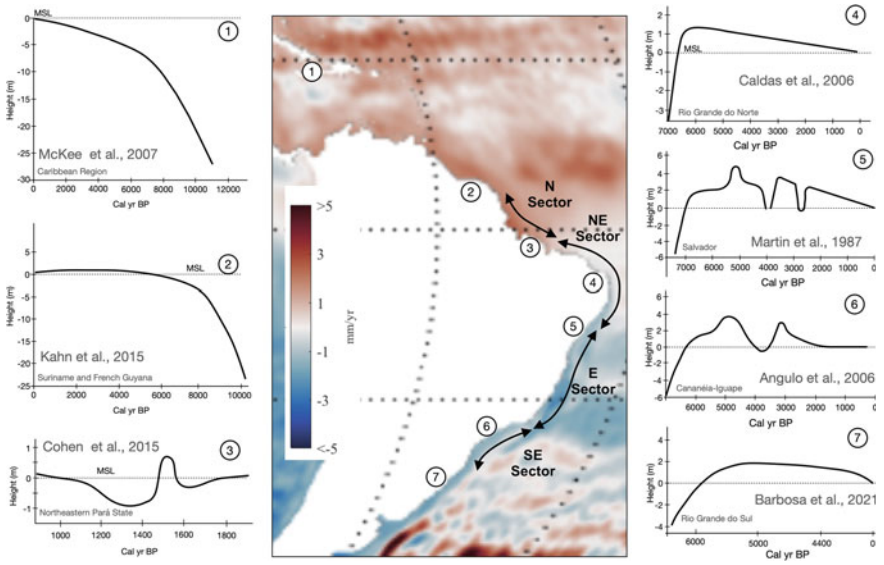

Fig. 3.13 Sea-level behavior from 1993 to 2015 (Elipot 2020) (central panel) and sea-level curves for the last 10,000 years for different regions of South America and the Caribbean. Modified from Martin et al. (1987), Angulo et al. (2006), Caldas et al. (2006), McKee et al. (2007), Cohen et al. (2015), Khan et al. (2015), and Barboza et al. (2021)

ice sheet (AIS) adjustments (Oppenheimer et al. 2019). These same behaviors are mimicked by the modern global mean sea-level (Elipot 2020) (Fig. 3.13).

The mangrove response and corresponding stratigraphy associated with these two sea-level histories observed along the Brazilian coast are illustrated in Fig. 3.14. In the North Sector of the Brazilian coast (Fig. 3.14a), transgressive muddy (Subsector N1) and sandy (Subsector N3) deposits record the rapid rise of sea-level from the LGM to the Mid-Holocene, when the first mangrove deposits accumulated in open muddy banks (Subsector N1) and sheltered tidal flats behind barrier islands (Subsector N3). In Subsector N3, under conditions of an almost stable sea level, successive barriers emerged during the Holocene, allowing for tidal flat progradation resulting in a continuous mangrove belt (Fig. 3.14a) up to 36 km wide (Souza-Filho et al. 2009).

In the Northeast, East and Southeast sectors of the Brazilian coast (Fig. 3.14b), maximum mangrove development occurred around the Mid-Holocene highstand when large bays and estuaries were present in the coastal zone (Dominguez et al. 1987). As a result of the 3–4 m drop in relative sea-level since that time, many of these bays, lagoons and estuaries were infilled, and the shoreline prograded, forming beach-ridge terraces (Andrade et al. 2003; Dominguez et al. 1987). The exposed estuarine and lagoon sediments were replaced by freshwater swamp environments (Fig. 3.14b). From that point on, mangrove development became restricted to sheltered areas behind narrow elongated barrier islands.

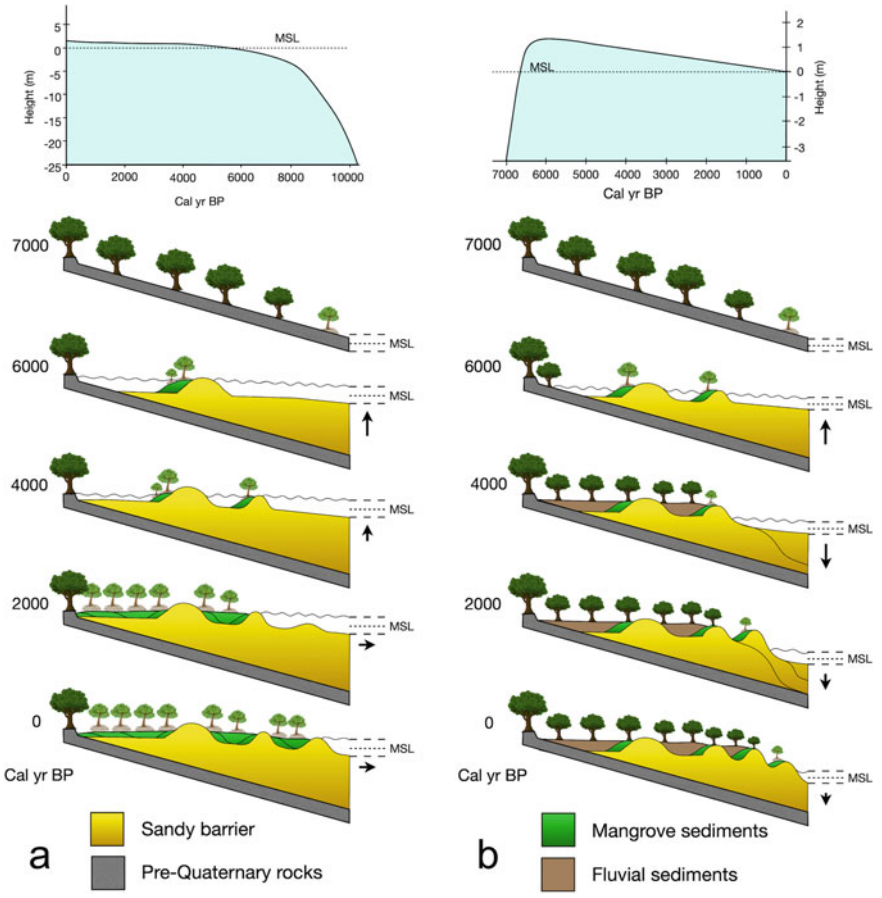

Fig. 3.14 Effects of different sea-level histories on the styles of mangrove sedimentation. **a** North Mangrove Sector and **b** Northeast, East, and Southeast Mangrove sectors

3.5.2 Impact of Future Sea-Level Rise in the Brazilian Mangroves

Mangrove sedimentation during the late Quaternary in response to postglacial sea-level rise brings important lessons as to how these ecosystems will respond to global warming and sea-level rise (SLR). Under the RCP8.5 scenario, the global mean sea-level (GMSL) will rise by 0.84 m (0.61–1.10 m) by 2100 (Oppenheimer et al. 2019). Beyond 2100, GMSL will continue to rise for centuries due to thermal expansion, mass loss of glaciers and ice sheets in the Greenland ice sheet (GIS) and Antarctic ice sheet (AIS) and land water storage changes.

The response of the mangrove coasts to this sea-level rise will depend on the environmental setting of the mangroves. Figure 3.15 presents four models of mangrove

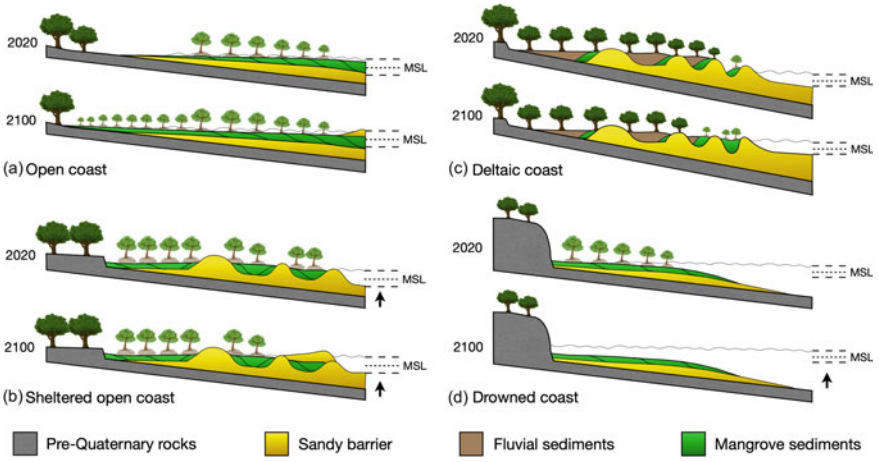

Fig. 3.15 Four response scenarios of mangrove sedimentation to ongoing sea-level rise

response to sea-level rise based on their past response to changes in hydrogeomorphic processes and pristine geological conditions, including changes in relative sea level.

On open coasts, a rise in sea-level will cause an increase in upstream penetration of the salt wedge and landward migration of mangroves along riverine and supratidal flats that are progressively converted to intertidal flats (Fig. 3.15a). Hence, mangrove zones migrate landward by seedling recruitment and vegetative reproduction as new brackish habitat becomes available landward through inundation and concomitant changes in salinity, as observed along the Australian coast (Semeniuk 1994). Erosive processes at the seaward front can result in mangrove loss along the shoreline (Allison et al. 2000; Anthony et al. 2010; Santos et al. 2016).

If sea-level is rising over a sheltered open coast densely colonized by mangroves and bounded landward by inactive cliffs, the muddy tidal flat will experience an elevation in the water level and a sedimentary aggradation process. Under this hydromorphic condition, the inner tidal flat may also expand laterally, prograding toward the estuarine channels and tidal creeks. The landward retreat of the shoreline due to the rising sea-level will result in barrier sand deposition over muddy flats and mangroves (Fig. 3.15b). This will cause coastal erosion, falling of trees, increased salinity, and hydroperiod, frequency, and depth of inundation in mangrove forests (Souza-Filho and Paradella 2003; Souza-Filho et al. 2006).

Along deltaic coasts (Fig. 3.15c), sea-level rise will result in increased salt wedge penetration and landward retreat of beach-dune ridges, occasionally burying tidal muddy flats colonized by mangroves. Mangrove survival will depend on the ability of mangrove species to colonize newly available habitats at a rate that keeps pace with the rate of sea-level rise. Hence, it might be possible to see a progressive landward migration of mangrove trees over deltaic flood plain deposits due to increased salinity.

Tropical tidal flats fringing high gradient land regions or human-made obstacles such as seawalls and other shoreline protection structures (Fig. 3.15d) will contain the mangroves most threatened by sea-level rise. They will be very likely drowned "in place" due to a lack of low-lying areas over which they can migrate. Hence, the mangroves situated in the Southeast Sector of the Brazilian coast, bounded by highland areas, are the ones most threatened by a rise in sea level. Nevertheless, the presence of construction, such as dams, roads, and seawalls, common along the Northeast and East sectors, may increase the vulnerability of mangroves to the rise in sea-level in those sectors (Lacerda et al. 2021).

3.6 Concluding Remarks

Brazil hosts the second largest mangrove area in the world. Mangroves develop around the mean sea-level and as such are potentially vulnerable to the impacts of the ongoing rise in sea level, which will certainly affect their distribution, structure, and function, and also impacting their dynamics, health and connectivity with adjacent systems.

Potential changes in the mangrove ecosystem will directly affect key factors that determine the survivability of mangrove forests. Such factors are related to abiotic processes, such as geomorphology and stratigraphy (Ellison and Stoddart 1991), topography, mineralogy and sedimentation (Woodroffe 1995), nutrient distribution and microclimate (Ellison 2000), and salt and freshwater in adjacent environments (Gilman et al. 2008).

Mangroves occupy almost the entire coastline of Brazil and developed under different environmental conditions. Four large coastal sectors were identified in which mangrove forests occur: North, Northeast, East, and Southeast (Fig. 3.1), each characterized by different geological-geomorphological, oceanographic, and climatic conditions.

Even in the face of a climate change scenario and a trend of sea-level rise over the last century, the Brazilian mangrove forest area has increased from 9564 km^2 in 1985 to 9800 km^2 in 2020, which represents an increase of 2.5%. In the North Sector on the Amazon coast, which is dominated by macrotides with a monsoon climate, the mangrove forest area represents 74.3% of the Brazilian mangroves. In the Northeast Sector, a mesotidal coast with a tropical savanna climate, mangrove areas compose 10.7% of the Brazilian mangroves. The East Sector, a meso- to microtidal coast with a humid tropical climate, encompasses 9.7% of the Brazilian mangroves. The Southeast Sector, a microtidal coast with a temperate oceanic climate, contains only 5.4% of the Brazilian mangroves.

The paleoenvironmental records of sea-level changes during the Holocene indicate that over millennial timescales, mangrove shorelines in the North sector were exposed to a continuous sea-level rise, while in the Northeast, East, and Southeast sectors, the sea-level trajectories were completely different, with a highstand at approximately 6000–7000 Cal year. BP followed by a 3- to 4-m sea-level drop. These

records point to a broad capacity of mangroves to adjust to sea-level changes. Four models of mangrove response to the ongoing rise in sea-level are proposed based on the understanding of past mangrove evolution under these varying Holocene sea-level histories. However, given the biogeographic variability of mangroves and environmental conditions along the Brazilian coast, predicting the effect of sea-level rise for the different mangrove sectors described herein is still a challenge. Further research is still needed to distinguish the effects of different phenomena and trends other than sea-level rise, which may affect mangroves on a multidimensional scale.

Acknowledgements We gratefully acknowledge the Conselho Nacional de Desenvolvimento Científico e Tecnológico (CNPq), Coordenação de Aperfeiçoamento de Pessoal de Nível Superior (CAPES), Mapbiomas, and Instituto Tecnológico Vale for the support provided to our research on Brazilian mangrove dynamics and evolution.

References

Allison MA, Nittrouer CA, Faria LEC (1995) Rates and mechanisms of shoreface progradation and retreat downdrift of the Amazon river mouth. Mar Geol 125(3–4):373–392. https://doi.org/10.1016/0025-3227(95)00020-Y

Allison MA, Lee MT, Ogston AS et al (2000) Origin of Amazon mudbanks along the northeastern coast of South America. Mar Geol 163:241–256. https://doi.org/10.1016/0025-3227(95)00020-Y

Almeida FFM, Carneiro CDR (1998) Origem e evolução da Serra do Mar. Rev Bras Geoc 28(2):135–150

Alvares CA, Stape JL, Sentelhas PC et al (2013) Koppen's climate classification map for Brazil. Meteorol Z 22(6):711–728. https://doi.org/10.1127/0941-2948/2013/0507

Andrade ACS, Dominguez JML, Martin L et al (2003) Quaternary evolution of the Caravelas strandplain—Southern Bahia State—Brazil. An Acad Bras Cienc 75:357–382. https://doi.org/10.1590/S0001-37652003000300008

Angulo RJ, Lessa GC, Souza MCd (2006) A critical review of mid- to late-Holocene sea-level fluctuations on the eastern Brazilian coastline. Quat Sci Rev 25(5–6):486–506. https://doi.org/10.1016/j.quascirev.2005.03.008

Anthony EJ, Gardel A, Gratiot N et al (2010) The Amazon-influenced muddy coast of South America: a review of mud-bank-shoreline interactions. Earth-Sci Rev 103(3–4):99–121. https://doi.org/10.1016/j.earscirev.2010.09.008

Barbirato JO, Ferreira NC, Zandonadi DB et al (2021) Structural characterization of areas with different levels of conservation in the mangrove of Vitória Bay, ES. Braz J Anim Environ Res 4(2):2600–2614. https://doi.org/10.34188/bjaerv4n2-085

Barboza EG, Dillenburg SR, do Nascimento Ritter M et al (2021) Holocene sea-level changes in southern brazil based on high-resolution radar stratigraphy. Geosciences 11(8):2600–2614. https://doi.org/10.3390/geosciences11080326

Barreto AMF, Suguio K, Bezerra FHR et al (2006) Geologia e Geomorfologia do Quaternário Costeiro do Estado do Rio Grande do Norte. Rev Inst Geoc USP 4(2):1–12

Batista EM, Souza-Filho PWM, Silveira OFM (2009) Avaliação de áreas deposicionais e erosivas em cabos lamosos da zona costeira Amazônica através da análise multitemporal de imagens de sensores remotos. Rev Bras Geof 27:83–96. https://doi.org/10.1590/S0102-261X2009000500007

Bezerra FHR, Barreto AMF, Suguio K (2003) Holocene sea-level history on the Rio Grande do Norte State coast Brazil. Mar Geo 196(1–2):73–89

Bezerra FHR, Amaro VE, Vita-Finzi C et al (2001) Pliocene-Quaternary fault control of sedimentation and coastal plain morphology in NE Brazil. J South Am Earth Sci 14(1):61–75. https://doi.org/10.1016/S0025-3227(03)00044-6

Bunting P, Rosenqvist A, Lucas MR et al (2018) The global mangrove watch—a new 2010 global baseline of mangrove extent. Remote Sens 10. https://doi.org/10.3390/rs10101669

Caldas LHdO, Stattegger K, Vital H (2006) Holocene sea-level history: evidence from coastal sediments of the northern Rio Grande do Norte coast NE Brazil. Mar Geol 228(1–4):39–53. https://doi.org/10.1016/j.margeo.2005.12.008

Cohen MCL, Alves ICC, França MC et al (2015) Relative sea-level and climatic changes in the Amazon littoral during the last 500years. CATENA 133:441–451. https://doi.org/10.1016/j.catena.2015.06.012

Costa BCF, Amaro VE, Ferreira ATS (2017) Classificação de Espécies de Mangue no Nordeste do Brasil com Base em Imagens Híbridas de Sensoriamento Remoto. Anu Inst Geoc—UFRJ 40(1):135–149. https://doi.org/10.11137/2017_1_135_149

Dadalto TP, Carvalho BC, Guerra JV et al (2022) Holocene morpho-sedimentary evolution of Marambaia Barrier Island (SE Brazil). Quat Res 105:182–200. https://doi.org/10.1017/qua.2021.43

Diniz C, Cortinhas L, Nerino G et al (2019) Brazilian mangrove status: three decades of satellite data analysis. Remote Sens 11. https://doi.org/10.3390/rs11070808

Doerffer R, Schiller H (2007) The MERIS Case 2 water algorithm. Int J Remote Sens 28(3–4):517–535. https://doi.org/10.1080/01431160600821127

Dominguez JML (2009) The Coastal Zone of Brazil. In: Dillenburg SF, Hesp PA (eds) Geology and Geomorphology of Holocene Coastal Barriers of Brazil. Springer, New York, pp 17–51. https://doi.org/10.1007/978-3-540-44771-9_2

Dominguez JML, Guimarães JK (2021) Effects of Holocene climate changes and anthropogenic river regulation in the development of a wave-dominated delta: The São Francisco River (eastern Brazil). Mar Geol 435. https://doi.org/10.1016/j.margeo.2021.106456

Dominguez JML, Martin L, Bittencourt ACSP (1987) Sea-level history and quaternary evolution of river-mouth-associated beach-ridge plains along the eastern/southeastern Brazilian coast: a summary. In: Nummedal D, Pilkey OH, Howard JD (eds) Sea-level fluctuation and coastal evolution. SEPM, Tulsa, Oklahoma, U.S.A., pp 115–127. https://doi.org/10.2110/pec.87.41.0115

Dominguez JML, Silva RP, Nunes AS et al (2013) The narrow, shallow, low-accommodation shelf of central Brazil: sedimentology, evolution and human uses. Geomorphology 203(1):46–59. https://doi.org/10.1016/j.geomorph.2013.07.004

Duke N, Ball M, Ellison J (1998) Factors influencing biodiversity and distributional gradients in mangroves. Glob Ecol Biogeogr Let 7(1):27–47. https://doi.org/10.2307/2997695

Duncan C, Owen HJF, Thompson JR et al (2018) Satellite remote sensing to monitor mangrove forest resilience and resistance to sea level rise. Methods Ecol Evol 9(8):1837–1852. https://doi.org/10.1111/2041-210X.12923

Elipot S (2020) Measuring global mean sea level changes with surface drifting buoys. Geophys Res Lett 47(21):e2020GL091078. https://doi.org/10.1029/2020GL091078

Ellison JC (2000) How South Pacific Mangroves may respond to predicted climate change and sea-level rise. In: Gillespie A, Burns WCG (ed) Climate change in the South Pacific: impacts and responses in Australia, New Zealand, and Small Island States, vol 2, advances in global change research. Springer, Dordrecht, pp 289–300. https://doi.org/10.1007/0-306-47981-8_16

Ellison JC (2015) Vulnerability assessment of mangroves to climate change and sea-level rise impacts. Wetl Ecol Manag 23(2):115–137. https://doi.org/10.1007/s11273-014-9397-8

Ellison JC, Stoddart DR (1991) Mangrove ecosystem collapse during predicted sea-level rise: Holocene analogues and implications. J Coast Res 7:151–165

Ferreira AV Jr, Paes BrCE, Vieira MM et al (2018) Diagenesis of Holocene Beachrock in Northeastern Brazil: petrology, isotopic evidence and age. Quat Environ Geosci. https://doi.org/10.5380/abequa.v9i2.53011

França CF, Souza-Filho PWM (2003) Análise das mudanças morfológicas costeiras de médio período na margem leste da Ilha de Marajó (PA) em Imagem Landsat. Rev Bras Geoc 32 (Suplemento 2):127–136

França CF, Souza-Filho PWM (2006) Compartimentação morfológica da margem leste da Ilha de Marajó: zona costeira dos municípios de Soure e Salvaterra—Estado do Pará. Rev Bras Geomorf 7(1):33–42

França CF, Souza-Filho PWM, El-Robrini M (2007) Análise faciológica e estratigráfica da planície costeira de Soure (margem leste da ilha de Marajó-PA), no trecho compreendido entre o canal do Cajuúna e o estuário Paracauari. Acta Amazonica 37(2):261–268. https://doi.org/10.20502/rbg.v7i1.58

Freitas H, Guedes MLS, Smith DH et al (2002) Characterization of the mangrove plant community and associated sediment of Todos os Santos Bay, Bahia Brazil. Aquat Ecosyst Health Manag 5(2):217–229. https://doi.org/10.1080/14634980290031901

Gilman EL, Ellison J, Duke NC et al (2008) Threats to mangroves from climate change and adaptation options: a review. Aquat Bot 89(2):237–250. https://doi.org/10.1007/s10661-006-9212-y

Giri C, Ochieng E, Tieszen LL et al (2011) Status and distribution of mangrove forests of the world using earth observation satellite data. Glob Ecol Biogeogr 20(1):154–159. https://doi.org/10.1111/j.1466-8238.2010.00584.x

Gomes Tapias J, Schobbenhaus C, Montez Ramírez NE (2019) Geological map of South America. In. CGMW, Servicio Geológico Colombiano, CPRM, Rio de Janeiro. https://rigeo.cprm.gov.br/handle/doc/21606

Halla MMS, Dominguez JML, Corrêa-Gomes LC (2020) Structural controls on the morphology of an extremely narrow, low-accommodation, passive margin shelf (Eastern Brazil). Geo-Mar Lett. https://doi.org/10.1007/s00367-019-00605-y

Hersbach H, Bell B, Berrisford P et al (2020) The ERA5 global reanalysis. Quarterly J Royal Meteorol Soc 146(730):1999–2049. https://doi.org/10.1002/qj.3803

Hesp PA, Maia LP, Claudino-Sales V (2009) The Holocene Barriers of Maranhão, Piauí and Ceará States, Northeastern Brazil. In: Dillenburg SF, Hesp PA (eds) Geology and geomorphology of holocene coastal barriers of Brazil. Springer, New York, pp 325–345. https://doi.org/10.1007/978-3-540-44771-10

IBGE (2020) Anuário estatístico do Brasil. Instituto Brasileiro de Geografia e Estatística, Rio de Janeiro—IBGE 80:1-1—8-50

Khan NS, Ashe E, Shaw TA et al (2015) Holocene relative sea-level changes from near-, intermediate-, and far-field locations. Curr Clim Change Rep 1(4):247–262. https://doi.org/10.1007/s40641-015-0029-z

Klein AHF, Short AD (2016) Brazilian beach systems: introduction. In: Short AD, Klein AHF (eds) Brazilian beach systems. Springer, Switzerland, pp 1–35. https://doi.org/10.1007/978-3-319-30394-9_1

Knoppers B, Ekau W, Figueiredo AG (1999) The coast and shelf of east and northeast Brazil and material transport. Geo-Mar Lett 19(3):171–178. https://doi.org/10.1007/s003670050106

Lacerda LD, Ward RD, Godoy MDP et al (2021) 20-Years cumulative impact from shrimp farming on mangroves of Northeast Brazil. Front For Glob Change. https://doi.org/10.3389/ffgc.2021.653096

Lessa GC, Santos FM, Souza Filho PW et al (2018) Brazilian estuaries: a geomorphologic and oceanographic perspective. In: Lana PdC, Bernardino AF (eds) Brazilian estuaries: a benthic perspective. Springer International Publishing, Cham, pp 1–37. https://doi.org/10.1007/978-3-319-77779-5_1

Locarnini RA, Mishonov AV, Baranova OK et al (2019) World Ocean Atlas 2018. In: Mishonov A (ed) vol NOAA Atlas NESDIS 81. NOAA, Silver Spring, MD, p 52. http://www.nodc.noaa.gov/OC5/indprod.html

Magris RA, Barreto R (2010) Mapping and assessment of protection of mangrove habitats in Brazil. Pan-Am J Aquat Sci 5(4):546–556

Martin L, Suguio K, Flexor J-M et al (1987) Quaternary evolution of the central part of the Brazilian coast. The role of relative sea-level variation and of shoreline drift. In: UNESCO (ed) Quaternary coastal geology of West Africa and South America. vol UNESCO Report in Marine Science. UNESCO, Paris, pp 97–145

McKee KL, Cahoon DR, Feller IC (2007) Caribbean mangroves adjust to rising sea level through biotic controls on change in soil elevation. Glob Ecol Biogeogr 16(5):545–556. https://doi.org/10.1111/j.1466-8238.2007.00317.x

McKee K, Rogers K, Saintilan N (2012) Response of Salt Marsh and Mangrove Wetlands to Changes in Atmospheric CO_2, Climate, and Sea Level. In: Middleton BA (ed) Global change and the function and distribution of Wetlands. Springer Netherlands, Dordrecht, pp 63–96. https://doi.org/10.1007/978-94-007-4494-3_2

Menezes MPMd, Berger U, Mehlig U (2008) Mangrove vegetation in Amazonia: a review of studies from the coast of Pará and Maranhão States, north Brazil. Acta Amazonica 38:403–420. https://doi.org/10.1590/S0044-59672008000300004

Nascimento WR Jr, Souza-Filho PWM, Proisy C et al (2013) Mapping changes in the largest continuous Amazonian mangrove belt using object-based classification of multisensor satellite imagery. Estuar Coast Shelf Sci 117:83–93. https://doi.org/10.1016/j.ecss.2012.10.005

Oppenheimer M, Glavovic BC, Hinkel J et al (2019) Sea level rise and implications for low-lying islands, coasts and communities. In: IPCC special report on the ocean and cryosphere in a changing climate. In: Pörtner HO, Roberts DC, Masson-Delmotte V et al (eds) Cambridge University Press, Cambridge UK-NY, USA, pp 321–445. https://doi.org/10.1017/9781009157964.006

Perry CT, Berkeley A, Smithers SG (2008) Microfacies characteristics of a tropical, mangrove-fringed shoreline, Cleveland Bay, Queensland, Australia: sedimentary and taphonomic controls on mangrove facies development. J Sediment Res 78(2):77–97. https://doi.org/10.2110/jsr.2008.015

Peulvast J-P, Sales VC, Bezerra FHR et al (2006) Landforms and neotectonics in the equatorial passive margin of Brazil. Geodin Acta 19(1):51–71. https://doi.org/10.3166/ga.19.51-71

Rodrigues SWP (2014) Detecção de mudança e sedimentação no estuário do rio Coreaú. In: Geoscience Institute. vol CDD 22. ed. 621.3678098131. Universidade Federal do Pará, Belém-PA, Brazil p 107

Rossetti DF (2014) The role of tectonics in the late Quaternary evolution of Brazil's Amazonian landscape. Earth-Sci Rev 139:362–389. https://doi.org/10.1016/j.earscirev.2014.08.009

Rossetti DF, Bezerra FHR, Dominguez JML (2013) Late Oligocene-Miocene transgressions along the equatorial and eastern margins of Brazil. Earth-Sci Rev 123:87–112. https://doi.org/10.1002/jqs.1132

Rossetti DF, Góes AM, Valeriano MM et al (2008) Quaternary tectonics in a passive margin: Marajó Island, northern Brazil. J Quat Sci 23(2):121–135. https://doi.org/10.1002/jqs.1132

Santos VF, Short AD, Mendes AC (2016) Beaches of the Amazon coast: Amapá and West Pará. In: Short AD, Klein AHF (eds) Brazilian beach systems. Coastal Research Library, Springer, Switzerland, pp 67–94. https://doi.org/10.1007/978-3-319-30394-9_3

Schaeffer-Novelli Y, Cintron-Molero G, Soares MLG (2002) Mangroves as indicators of sea level change in the muddy coasts of the world. In: Healy T, WaJ-AH Y (ed) Muddy coasts of the world: processes, deposits and function. Springer, New York, pp 245–262. https://doi.org/10.1016/S1568-2692(02)80083-3

Schaeffer-Novelli Y, Cintrón-Molero G, Adaime R et al (1990) Variability of mangrove ecosystems along the Brazilian coast. Estuaries Coast 13(2):204–218. https://doi.org/10.2307/1351590

Semeniuk V (1994) Predicting the effect of sea-level rise on mangroves in Northwestern Australia. J Coast Res 10(4):1050–1076

Semeniuk V (2018) Tidal flats. In: Finkl CW, Makowski C (eds) Encyclopedia of coastal science. Springer International Publishing, Cham, pp 1–20. https://doi.org/10.1007/978-3-319-48657-4_317-2

Silva JB, Torres MFA (2021) Assinatura Energética dos Manguezais no Domínio Costeiro Brasileiro. Rev Bras Geogr Fís 14(4):2286–2303. https://doi.org/10.26848/rbgf.v14.4.p2286-2303

Soares MLG, Estrada GCD, Fernandez V et al (2012) Southern limit of the Western South Atlantic mangroves: assessment of the potential effects of global warming from a biogeographical perspective. Estuar Coast Shelf Sci 101:44–53. https://doi.org/10.1016/j.ecss.2012.02.018

Souza-Filho PWM (2000) Tectonic control on the coastal zone geomorphology of the northeastern Pará State. Rev Bras Geoc 30(3):523–526

Souza-Filho PWM (2005) Costa de manguezais de macromaré da Amazônia: cenários morfológicos, mapeamento e quantificação de áreas usando dados de senores remotos. Rev Bras Geof 23(4):427–435. https://doi.org/10.1590/S0102-261X2005000400006

Souza-Filho PWM, Paradella WR (2003) Use of synthetic aperture radar for recognition of Coastal Geomorphological Features, land-use assessment and shoreline changes in Bragança coast, Pará Northern Brazil. Acad Bras Cienc 75(3):341–356. https://doi.org/10.1590/S0001-37652003000300007

Souza-Filho PWM, Farias Martins EdS, Costa FR (2006) Using mangroves as a geological indicator of coastal changes in the Bragança macrotidal flat, Brazilian Amazon: a remote sensing data approach. Ocean Coast Manag 49(7–8):462–475. https://doi.org/10.1016/j.ocecoaman.2006.04.005

Souza-Filho PWM, Paradella WR, Silveira OFM (2005) Synthetic aperture radar for recognition of coastal features in the wet tropics: apllications in the Brazilian Amazon coast. Bol Mus Para Emílio Goeldi. Ser Ciênc Nat 1(1):201–207

Souza-Filho PWM, Lessa GC, Cohen MCL et al (2009) The subsiding macrotidal barrier estuarine system of the Eastern Amazon coast, Northern Brazil. In: Dillenburg SF, Hesp PA (eds) Geology and geomorphology of holocene coastal barriers of Brazil. Springer, New York, pp 347–375. https://doi.org/10.1007/978-3-540-44771-9

Stramski D, Reynolds RA, Babin M et al (2008) Relationships between the surface concentration of particulate organic carbon and optical properties in the eastern South Pacific and eastern Atlantic Oceans. Biogeosciences 5(1):171–201. https://doi.org/10.5194/bg-5-171-2008

Tomlinson PB (2016) The botany of mangroves. Cambridge University Press, Cambridge. https://doi.org/10.1017/CBO9781139946575

Vieira MM, Sial AN, De Ros LF et al (2017) Origin of holocene beachrock cements in northeastern Brazil: evidence from carbon and oxygen isotopes. J South Am Earth Sci 79:401–408. https://doi.org/10.1016/j.jsames.2017.09.002

Vital H, Silveira IM, Tabosa WF et al (2016) Beaches of Rio Grande do Norte. In: Short AD, Klein AHF (eds) Brazilian Beach Systems. Coastal Research Library, vol Coastal Research Library. Springer, Switzerland, pp 200–229. https://doi.org/10.1007/978-3-319-30394-9_8

Woodroffe CD (1995) Response of tide-dominated mangrove shorelines in Northern Australia to anticipated sea-level rise. Earth Surf Process Landf 20(1):65–85. https://doi.org/10.1002/esp.3290200107

Woodroffe CD (2018) Mangrove response to sea level rise: palaeoecological insights from macrotidal systems in northern Australia. Mar Freshw Res 69(6):917–932. https://doi.org/10.1071/MF17252

Woodroffe CD (2019) Chapter 2—the morphology and development of coastal wetlands in the tropics. In: Perillo GME, Wolanski E, Cahoon DR et al (eds) Coastal Wetlands, 2nd edn. Elsevier, pp 79–103. https://doi.org/10.1016/B978-0-444-63893-9.00002-2

Woodroffe CD, Rogers K, McKee KL et al (2016) Mangrove sedimentation and response to relative sea-level rise. Annu Rev Mar Sci 8(1):243–266. https://doi.org/10.1146/annurev-marine-122414-034025

Worthington TA, zu Ermgassen PSE, Friess DA, et al (2020) A global biophysical typology of mangroves and its relevance for ecosystem structure and deforestation. Sci Rep 10(1):14652. https://doi.org/10.1038/s41598-020-71194-5

Zweng MM, Reagan JR, Seidov D et al (2018) World Ocean Atlas, volume 2: Salinity. In: Mishonov A (ed) vol NOAA Atlas NESDIS 82. NOAA/NESDIS, Silver Spring, MD. p 50. http://www.nodc.noaa.gov/OC5/indprod.html